Journal of Biomolecular NMR, **25:** 153–156, 2003.
KLUWER/ESCOM

Letter to the Editor: NMR structure of ubiquitin-like domain in PARKIN: Gene product of familial Parkinson's disease

Mitsuru Tashiro[a], Seiji Okubo[b], Sakurako Shimotakahara[b,c], Hideki Hatanaka[c], Hideyo Yasuda[d], Masatsune Kainosho[a], Shigeyuki Yokoyama[c,e,f] & Heisaburo Shindo[b,c,*]

[a]*Department of Chemistry, Faculty of Science, Tokyo Metropolitan University, Minami-osawa, Hachioji, Tokyo 192-0367, Japan;* [b]*School of Pharmacy and* [d]*School of Life Science, Tokyo University of Pharmacy & Life Science, Horinouchi, Hachioji, Tokyo 192-0392, Japan;* [c]*Genomic Sciences Center, RIKEN, Suehiro-cho, Tsurumi-ku, Yokohama 230-0045, Japan;* [e]*Harima Institute at SPring-8, RIKEN, Mikazuki-cho, Sayo, Hyogo 679-5148, Japan;* [f]*Department of Biophysics and Biochemisty, Graduate School of Science, The University of Tokyo, Hongo, Bunkyo-ku, Tokyo 110-0033, Japan*

Received 28 August 2002; Accepted 30 October 2002

Key words: NMR structure, PARKIN, Parkinson's disease, ubiquitin

Biological context

The gene product, PARKIN, has been identified as the major cause of autosomal recessive juvenile parkinsonism (AR-JP) resulting from the mutations of *PARK2* (Kitada et al., 1998). In AR-JP patients, the loss of dopaminergic neurons and consequently the development of parkinsonian syndromes can occur without intracytoplasmic-ubiquitinated inclusion (i.e., Lewy body formation) (Mizuno et al., 1998). PARKIN has been identified as ubiquitin ligase E3, and the mutant PARKINs from AR-JP patients show loss of the ubiquitin ligase activity (Shimura et al., 2000). The murine PARKIN is composed of 464 amino acids with 83.2% identity to human Parkin and characterized by three domains: an N-terminal ubiquitin-like domain (Uld), and two RING finger-like domains, RING1 and RING2 (Kitada et al., 2000). Thus, PARKIN is classified into the RING-motif ubiquitin ligase E3 family.

A dozen PARKIN-like proteins possessing ubiquitin-like domains (Uld) which mediate a wide range of cellular functions (Jentsch and Pyrowolakis, 2000). The three-dimensional structures of the Uld of hPLIC-2 and hHR23a (Walters et al., 2002), and also of UBX (Buchberger et al., 2001) have recently been determined, and were found to be very similar to that of human ubiquitin, although there were substantial differences with regard to the potential surface, suggesting that the Uld plays important roles in specific protein-protein interactions. To elucidate the specific role of the Uld in PARKIN, we have constructed the deletion mutant of murine PARKIN that contains Uld alone, and determined its solution NMR structure. The structure determined here was found to have a ubiquitin fold, which not only provides functional versatility of the ubiquitin-like domain but also sheds light on the origin of parkinsonism.

Methods and results

The recombinant murine Uld was expressed as an inclusion body in *E. coli* strain BL21(DE3) grown in M9 medium using the expression vector pET28b (Novagen). The sonicated cell lysate was centrifuged and the precipitate was dissolved in 6 M guanidine hydrochloride and sequentially dialyzed against 3-0 M guanidine hydrochloride in 25 mM acetate buffer at pH 5.0. The protein was purified on an SP-Sepharose cation exchange column (Amersham Biosciences), followed by gel filtration chromatography on a Superdex-75 column (Amersham Biosciences). All NMR spectra were acquired at 25 °C on a Bruker DMX-500, DRX-600, Varian Inova-600 or Varian Inova-800 spectrometers. The standard triple-resonance methodology was employed to obtain sequential backbone and side-chain assignments for ca. 1 mM sample of ^{13}C /^{15}N- or ^{15}N-uniformly

*To whom correspondence should be addressed. E-mail: shindo@ps.toyaku.ac.jp

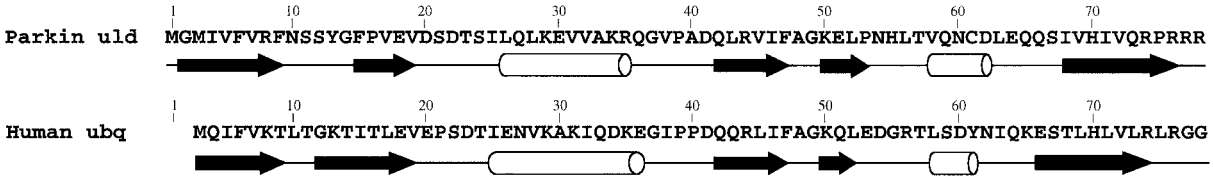

Figure 1. Comparison of the amino acid sequence and the secondary structural elements between murine Uld and human ubiquitin.

labeled Uld protein in 25 mM C^2H_3COONa, 2 mM dithiothreitol-d_{10} and 10% ^2H_2O at pH 5.0. The spectra were processed with NMRPipe (Delaglio et al., 1995) and analyzed with SPARKY (Goddard and Kneller). The structure calculations and refinement were performed with X-PLOR v.3.1 (Brunger, 1992). The complete backbone assignments were made using a pair of CBCA(CO)NH and CBCANH experiments, and verified using a HNCA experiment. The nearly complete assignments of the side-chain ^1H and ^{13}C resonances were made using H(CCO)NH, HCCH-TOCSY and C(CO)NH data sets. The ^1H, ^{13}C, and ^{15}N chemical shifts were referenced to DSS according to the IUPAC recommendation (Markley et al., 1998), and have been deposited in the BioMagResBank (accession code BMRB-5496).

The analyses of ^{13}C- and ^{15}N-edited NOESY spectra were performed with in-house automated assignment program (Hatanaka et al., 1994) using the structure of human ubiquitin as distance filter only at the initial stage. A total of 604 NOEs (303 for intraresidue, 129 for sequential, 70 for medium-range and 102 for long-range) were thus obtained from the 3D ^{15}N- and ^{13}C-edited NOESY-HSQC spectra acquired with a mixing time of 75 ms in each experiment. It should be noted that the possible bias introduced by the initial usage of homology model in the analysis was small since the model structure used as an initial distance filter violates as much as 16% of the final long range NOE restraints by more than 3 Å (the largest violation is 9.9 Å).

The secondary structure of Uld in PARKIN, as determined by the consensus of the chemical shift index (Wishart and Sykes, 1994) and the patterns of successive $d_{\alpha N}$ and d_{NN} NOE connectivities, comprises five β-strands (residues 2–9, 15–19, 42–47, 50–54 and 68–76) and two helices (residues 26–35 and 58–62) (Figure 1). The global fold and the positioning of the secondary structural elements in Uld are similar to those of human ubiquitin as shown in Figures 1 and 2. Constraints for dihedral angles φ and ψ (41 for each) were obtained using the program TALOS (Cornilescu et al., 1999), and 30 hydrogen bonds were identified from $^1H/^2H$ exchange experiments. Using these constraints including 604 NOEs, simulated anealing and distance geometry calculations were performed. The statistics on the 10 conformers used to characterize the NMR structure are summarized in Table 1, and the superimposed backbone structures of Uld are shown in Figure 2a. As a whole, the NMR-derived structures of Uld are well-defined with a backbone rmsd-value of 0.50 Å for residues 4–73. The atomic coordinates have been deposited in the Protein Data Bank (PDB ID code 1mg8).

Table 1. Geometric statistics for the 10 final structures

R.m.s. deviation from idealized geometry		
Angles (°)	0.81	± 0.02
Bonds (Å)	0.0049	± 0.0003
Improper (°)	0.69	± 0.05
R.m.s. deviation from distance restraints (Å)	0.067	± 0.003
R.m.s. deviation from dihedral restraints (°)	5.56	± 0.25
R.m.s. deviation from the mean structure (Å)		
Backbone atoms (residues 4–73)	0.50	± 0.10
All heavy atoms (residues 4–73)	0.98	± 0.13
Ramachandran plot (%)		
Most favored region	74.6	
Allowed region	22.9	
Disallowed region	2.5	

Discussion and conclusions

As shown in the ribbon model in Figure 2a, Uld possesses a ββαββαβ secondary structure and the strands are arranged into a mixed five-stranded β-sheet in order 21534. The longer helix-1 packs across the concave sheet at angle about 50^o to the three strands, β-1, β-3 and β-5. The second helix is situated in the loop between strands 4 and 5. The overall structure of Uld is strikingly similar to that of human ubiquitin (Vijay-Kumar et al., 1987) with 1.38 Å r.m.s.d.

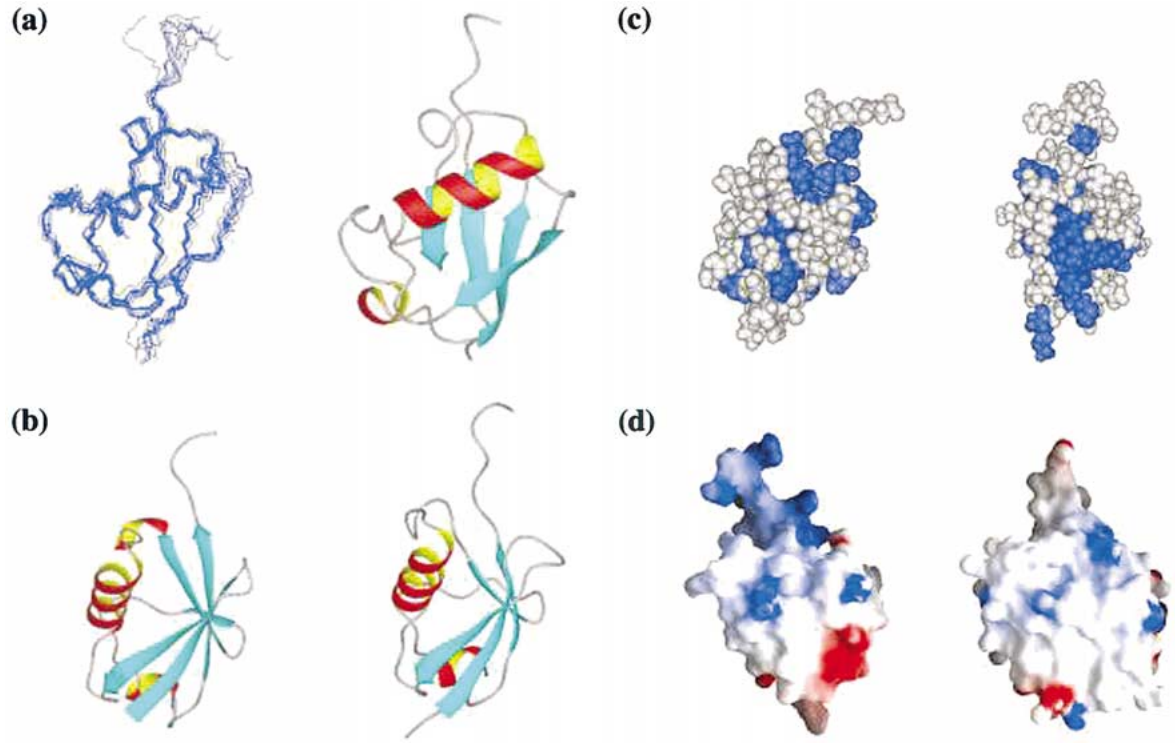

Figure 2. The solution structure of Uld and comparison with the crystallographic structure of human ubiquitin (PDB ID code 1UBQ). (a) Superimposed backbone atoms for 10 structures of Uld (left) and a ribbon diagram of the minimized average structure of Uld (right) in the same orientation. Residues 4–73 were used for the superposition. (b) Ribbon diagrams for Uld (left) and human ubiquitin (right). Structures are drawn using the program MOLMOL (Koradi et al., 1996). (c) Surface distribution of hydrophobic and aromatic residues for Uld (left) and human ubiquitin (right) are presented in the same orientation as (b). Hydrophobic and aromatic residues are colored blue, and the other residues are colored white. (d) Electrostatic potential surfaces of Uld (left) and human ubiquitin (right). The views represent 180° rotation of ribbon diagrams in (b). The program GRASP was used for construction of these figures (Nicholls et al., 1991).

for backbone atoms of residues 4–73 between two structures (Figure 2b).

A closer examination, however, reveals some significant differences in surface properties between two proteins. The hydrophobicity between Uld and human ubiquitin is compared in Figure 2c. A hydrophobic patch comprising residues I4, V5, F6, V7, F9, Y13, F15, P16 and V17, most of which are not present in human ubiquitin, is a characteristic feature of Uld. This hydrophobic patch is positioned in the region of strand-1 and strand-2 (see Figure 2c). The presence of this unique and prominent hydrophobic surface of Uld could account for noticeable instability in solution, and explain its tendency to aggregate within 10–14 days under the present solvent condition. Meanwhile, the electrostatic surface potential also reveals significantly different patterns between Uld and human ubiquitin. As can be seen in Figure 2d, a conspicuous cluster of negatively charged residues located at the lower bottom of Uld molecule is absent in human ubiquitin. This cluster is comprised from residues D62 and E64 corresponding to residues N60 and N62 in human ubiquitin which are both neutral residues. The rest of charge distributions is relatively similar between two proteins except the positively charged C-terminal region in Uld. In human ubiquitin, the C-terminal region ends with two glycine residues which contributes to polyubiquitination site, where these residues are absent in Uld. The arginine-rich motif at the C-terminus of Uld might be involved in the interaction with other protein/domain, playing a unique role in PARKIN. One possible such protein is *O*-glycosylated α-synuclein since it has been reported that only glycosylated α-synuclein was able to bind with Uld (Shimura et al., 2001).

Three human Parkin mutants, K29N, R44P and V58E, identified from AR-JP patients possess point mutations in the region of Uld domain (Hedrich et al., 2002; Hoenicka et al., 2002). It is worth noting that these three residues are conserved in human ubiqui-

tin as well as in murine PARKIN. Interestingly one charge is decreased in each mutant, which may cause serious changes in interaction with other residues. The residue K29 is involved in α-helix, and the close contact is observed between K29 and A40. As the length of the side chain is decreased by this mutation, the changes in the molecular packing as well as the charge distribution could have serious effects on molecular stability. The residue R44 is positioned in the middle of strand-3, and its amide proton forms a hydrogen bond with the backbone carbonyl oxygen of V72 in the opposite antiparallel strand-5 as identified through the analysis of hydrogen/deuterium exchange experiment and two interstrand NOEs between R44 H^N-V72 H^N, and R44 H^N-Q73 H^α. The mutation of arginine 44 to proline in Uld obviously destabilized the formation of β-sheet due to the lack of an amide proton in proline residue, leading to the elimination of one hydrogen bond. The residue V58 is located at the beginning of the short 3_{10} helix. The mutation of valine to glutamate can greatly alter the hydrophobic packing resulting in the destabilization of the overall conformation. In addition, two of the three conserved residues naturally mutated in human PARKIN, K29 and R44, are identical in human ubiquitin (K27 and R42). The other residue, V58, is a leucine (L56) in human ubiquitin, according to the alignment shown in Figure 1. It has been reported that K27 and L56 in human ubiquitin participate in hydrophobic core packing which governs overall stability of the protein (Lazar et al., 1997). Therefore, it is reasonable to presume that these mutations have a significant impact on the stability of Uld. And the destabilization of this domain by these mutations might lead to the elimination of ubiquitin ligase activity in the mutant proteins identified from AR-JP patients. We are currently further investigating these mutational effects.

In conclusion, the ubiquitin-like domain of murine PARKIN has a common motif of a ubiquitin fold, but considerably differs in its surface properties from human ubiquitin. This result implies that murine Uld is functionally different from human ubiquitin, perhaps serving as recognition domain for certain target proteins.

Acknowledgements

We thank Ms Yukiko Hachimori for her help in structural calculation and Dr William S. Price for useful discussion and critical reading of the manuscript. This work was supported by grants for Education and Science Research from the Promoting Agency for Private Schools, Japan to H.S. and by Grants-in-Aid for Basic Science Research (14572038) from the Ministry of Education, Science and Culture, Japan to H.S. This work was supported in part by National Project on Protein Structural and Functional Analyses.

References

Brunger, A.T. (1992) *X-PLOR, a System for X-ray Crystallography and NMR*, Yale University Press, New Haven.

Buchberger, A., Howard, M.J. and Proctor, M. (2001) *J. Mol. Biol.*, **307**, 17–24.

Delaglio, F., Grzesiek, S., Vuister, G., Zhu, W., Pfeifer, J. and Bax, A. (1995) *J. Biomol. NMR*, **6**, 277–293.

Goddard, T.D. and Kneller, D.G. *SPARKY 3*, University of California, San Francisco.

Hatanaka, H., Oka, M., Kohda, D., Tate, S., Suda, A., Tamiya, N. and Inagaki, F. (1994) *J. Mol. Biol.*, **240**, 155–166.

Hedrich, K., Marder, K., Harris, J., Kann, M., Lynch, T., Meija-Santana, H., Pramstaller, P.P., Schwinger, E., Bressman, S.B., Fahn, S. and Klein, C. (2002) *Neurology*, **58**, 1239–1246.

Hoenicka, J., Vidal, L., Morales, B., Ampuero, I., Jimenez-Jimenez, F.J., Berciano, J., del Ser, T., Jimenez, A., Ruiz, P.G. and de Yebenes, J.G. (2002) *Arch Neurol.*, **59**, 966–970.

Jentsch, S. and Pyrowolakis, G. (2000) *Trends Cell Biol.*, **10**, 335–342.

Kitada, T., Asakawa, S., Hattori, N., Matsumine, H., Yamamura, Y., Minoshima, S., Yokochi, M., Mizuno, Y. and Shimizu, N. (1998) *Nature*, **392**, 605–608.

Kitada, T., Asakawa, S., Minoshima, S., Mizuno, Y. and Shimizu, N. (2000) *Mamm. Genome*, **11**, 417–421.

Koradi, R., Billeter, M. and Wuthrich, W. (1996) *J. Mol. Graph.*, **14**, 51–55.

Lazar, G.A., Desjarlais, J.R. and Handel, T.M. (1997) *Protein Sci.*, **6**, 1167–1178.

Markley, J.L., Bax, A., Arata, Y., Hilbers, C.W., Kaptein, R., Sykes, B.D., Wright, P.E. and Wuthrich, K. (1998) *J. Mol. Biol.*, **280**, 933–952.

Mizuno, Y., Hattori, N. and Matsumine, H. (1998) *J. Neurochem.*, **71**, 893–902.

Nicholls, A., Sharp, K.A. and Honig, B. (1991) *Proteins*, **11**, 281–296.

Shimura, H., Hattori, N., Kubo, S., Mizuno, Y., Asakawa, S., Minoshima, S., Shimizu, N., Iwai, K., Chiba, T., Tanaka, K. and Suzuki, T. (2000) *Nat. Genet.*, **25**, 302–305.

Shimura, H., Schlossmacher, M.G., Hattori, N., Frosch, M.P., Trockenbacher, A., Schneider, R., Mizuno, Y., Kosik, K.S. and Selkoe, D.J. (2001) *Science*, **293**, 263–269.

Vijay-Kumar, S., Bugg, C.E. and Cook, W.J. (1987) *J. Mol. Biol.*, **194**, 531–544.

Walters, K.J., Kleijnen, M.F., Goh, A.M., Wagner, G. and Howley, P.M. (2002) *Biochemistry*, **41**, 1767–1777.

Wishart, D.S. and Sykes, B.D. (1994) *J. Biomol. NMR*, **4**, 171–180.